2023 IEEE International Conference on Robotics and Automation (ICRA 2023)
May 29 - June 2, 2023. London, UK

Big data approach for synthesizing a spatial linkage mechanism *

Neung Hwan Yim, Jegyeong Ryu, and Yoon Young Kim

Abstract— **This paper presents a novel two-step method for synthesizing spatial linkage mechanisms. Compared with planar mechanisms, the main challenge in synthesizing spatial mechanisms is that the generating motion varies depending on its mechanism topologies. Therefore, we propose a big data approach to determine the topology of spatial mechanisms. We adopt a three-dimensional (3D) spring-connected rigid block model to represent the topology of the spatial mechanism and project 3D motion onto three orthogonal planes to determine the mechanism topology with big data. In addition, a gradient-based dimension synthesis procedure was carried out to determine a detailed dimension using already determined mechanism topology by mechanism big data. Also, several successful case studies by the proposed approach are presented to support the effectiveness of the proposed synthesis method.**

I. INTRODUCTION

A spatial mechanism can convert two-dimensional (2D) actuating movement into the desired three-dimensional (3D) motions at its end effector. Therefore, its topology and mechanism dimensions must be accurately determined to generate the desired motion. In a conventional motion-generating synthesis problem, the candidate topology of mechanisms should be selected before mechanism dimensions can be adjusted [1-3]. However, when choosing candidate mechanisms, engineers have generally depended on insight and experience or used a simple mechanism topology. By contrast, an adjacency matrix and graph theory can also be utilized to select the topology of a spatial mechanism [4, 5]. However, because these matrix-based topology synthesis methods cannot provide an initial configuration for determining the mechanism dimensions, the results cannot be directly used for dimensional synthesis. Therefore, there was no design method that could directly and systematically synthesize the topology and dimensions of the spatial linkage mechanism in motion generation synthesis problems. However, a ground model-based topology synthesis method combined with shape optimization, called mechanism topology optimization, has the advantage of systematically synthesizing a mechanism's topology and dimensions [6-10]. This is because ground structure models, such as the spring-connected rigid block model (SBM) [9-15] and the nonlinear bar model [6-8, 16], can represent both the topology and dimensions of the mechanism with a single unified method. Therefore, this study attempts to design a spatial linkage mechanism using a ground structure model that is advantageous for representing various type of mechanisms.

Gradient-based optimization should be used in the ground model-based mechanism topology optimization for managing design variables required to represent the topology and dimension of a mechanism [6-10, 12-14, 17, 18]. However, a high number of design variables can still create issues in ground model-based topology optimization, especially in a spatial linkage mechanism. To minimize the number of design variables in a ground model-based synthesis method, a two-step approach that first determines the topology design variables corresponding to the mechanism topology by mechanism big data has been successfully studied in a planar mechanism (gradient-based optimization is used in the following dimensional synthesis) [15]. Therefore, we propose a two-step method based on a neural network-based approach for systematically designing the topology and dimensions of spatial mechanisms.

The neural network-based approaches are efficient for nonlinear mapping and suitable for considering mechanism topology and initial configuration in a given target motion. However, there are challenges in proposing neural network-based methods for spatial linkage mechanisms. First, there is a need for a ground model representing various topologies and dimensions of the spatial linkage mechanism. To represent spatial mechanism in a single model, we used 3D SBM in this study [17]. In 3D SBM, the design domain of the spatial mechanism is discretized by 3D rigid blocks interconnected by artificial zero-length springs with variable stiffness. When the stiffness variables of each spring reach the upper or lower value, various mechanism topologies are represented. Moreover, various mechanism dimensions can be expressed in the shape of a 3D rigid block. Second, we have to represent the mechanism topology and its generating motion to efficiently train the neural network. In a previous study, Yim et al. [15] represented a 2D generating path as Fourier-transformed descriptors of the centroid distance function. Because the centroid distance function does not apply to 3D motions, we project the 3D motion onto three orthogonal planes and then express them with the Fourier-transformed descriptors of the centroid distance function, as shown in the upper left of Fig. 1. Third, unlike planar mechanisms, various rotational angles and joint types (spherical, revolute, and universal) exist in the spatial mechanism. For this reason, it is difficult to interpolate the relationship between generating motion and mechanism topology when representing mechanism topology using spring stiffness values by neural networks. To overcome these limitations, instead of interpolating the stiffness values of the springs directly, we attempt to synthesize the mechanism topology as a multi-class classification problem by defining the class number corresponding to the mechanism topology (configuration).

* Research supported by Samsung Research Funding Center of Samsung Electronics (SRFC-IT1901-02) and National Research Foundation of Korea (2014M3A6B3063711 and 2022R1A2C2008067).

Neung Hwan Yim is with the Seoul National University, Seoul, Republic of Korea (corresponding author e-mail: leem0925@ snu.ac.kr).

Jegyeong Ryu is with Korea Institute of Science and Technology, Seoul, Republic of Korea (e-mail: ryujg@kist.re.kr).

Yoon Young Kim is with the Seoul National University, Seoul, Republic of Korea (e-mail: yykim@snu.ac.kr).

Now, we present an overall process of the proposed two-step approach, as shown in Fig. 1. However, we only consider the complete path: the corresponding mechanism should be a fully rotatable mechanism driven by a single driving actuator. In Step 1, the topology synthesis step, we determine a mechanism topology and initial configuration through a neural network-based approach for the subsequent dimensional synthesis step. To this end, it is important to efficiently generate many mechanism datasets to construct the neural network. The use of 3D SBM allows for an effective mechanism data generation scheme because various topologies and dimensions can be represented in a single model with a certain set of stiffness values and shape of rigid 3D blocks. In addition, mechanisms that are not physically feasible or do not allow full rotatability for a particular set of stiffness values can be filtered out by calculating the mean value of the work transmittance efficiency function [6]. Once the mechanism topology is determined, the shape optimization in the following dimensional synthesis step determines the detailed dimensions of the link.

II. GENERATING BIG DATA MECHANISM WITH 3D SBM

A. 3D SBM for unified spatial mechanism modeling

In this study, 3D SBM was utilized to generate a mechanism big data with various configurations (both topologies and dimensions). The 3D SBM method discretizes the design domain with 3D rigid blocks, which are interconnected by artificial zero-length springs [17]. Furthermore, each 3D rigid block and ground node are connected by a zero-length spring. In this study, the discretization resolution to the design domain was limited to 2 × 2 × 2 3D rigid blocks due to computational cost and time. Nevertheless, various mechanism configurations can be obtained with mechanism synthesis.

In 3D SBM, an interconnected zero-length spring with a maximum stiffness value represents a spherical joint (S), and a combination of spherical joints can represent various other joint types, as shown in Fig. 2. For example, if two spherical joints are connected between two adjacent blocks, a revolute joint (R) is represented. Moreover, the rotating axis of the revolute joint can be represented by the connecting line of two maximum springs. When four spherical joints connect two blocks at every node, the blocks are rigidly connected. Additionally, a universal joint (U) is represented when the rotating axes of two revolute joints meet at one node of the block. Therefore, as shown in Fig. 2, the 3D SBM can represent different joint types (revolute, spherical, and universal) with various combinations of spring stiffness. If necessary, it may be possible to include other joints such as prismatic and helical joints if more sophisticated spring components are used as done in 2D SBM [10, 12].

For convenience, each spring stiffness ($\mathbf{k}$) is normalized as $0 < \xi^K \le 1$, such that $\mathbf{k} = k_{\max} \cdot \left(\xi^K\right)^3$ ($k_{\max}$ is the designated maximum stiffness for the following analysis), as in previous studies [9, 12]. The vector symbol $\boldsymbol{\xi}^K$, used to represent the stiffness of all springs (both block-to-block and block-to-ground), is a topology design variable. $\boldsymbol{\xi}^K$ is either the lower bound (0) or upper bound (1) value, indicating the disconnection or connection state, respectively, between two rigid blocks or block and ground. Another set of design variables ($\boldsymbol{\xi}^X$), representing the 3D-block shapes, is used to determine the mechanism dimensions as real-valued values between 0 and 1.

Using randomly generated design variables $\boldsymbol{\xi}^K$ and $\boldsymbol{\xi}^X$ based on 3D SBM, the generating motion of the corresponding mechanism is obtained by the quasi-static force equilibrium. This quasi-static force equilibrium is based on each block's position and rotation angles, which is the state vector of 3D rigid block. For example, the state vector of the l^{th} rigid block ($\mathbf{q}_t^{(l)}$) at time step t can be represented with its center coordinates ($\left[X_t^{(l)}, Y_t^{(l)}, Z_t^{(l)}\right]$) and its angle of rotation ($\left[\theta_t^{(l)}, \varphi_t^{(l)}, \psi_t^{(l)}\right]$) in the global coordinate system:

$$\mathbf{q}_t^{(l)} = \left[X_t^{(l)}, Y_t^{(l)}, Z_t^{(l)}, \theta_t^{(l)}, \varphi_t^{(l)}, \psi_t^{(l)}\right]. \quad (1)$$

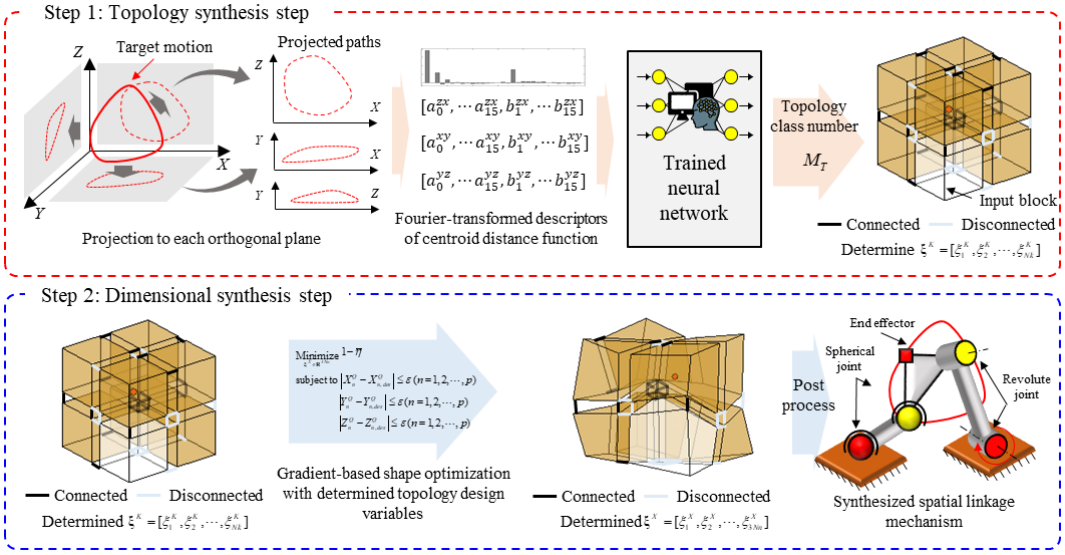

Figure 1. Overall process of synthesizing a spatial mechanism with proposed method.

The state vector of all 3D rigid blocks in the design domain, except for the input first rigid block, is expressed as the state variable vector $\mathbf{v}_t$ at t:

$$\mathbf{v}_t = \left[\left(\mathbf{q}_t^{(2)}\right)^T, \left(\mathbf{q}_t^{(2)}\right)^T, \cdots, \left(\mathbf{q}_t^{(8)}\right)^T \right]. \quad (2)$$

The quasi-static force equilibrium for generating motion with $\mathbf{v}_t$ can be written as:

$$\mathbf{F}_{\text{int},t}(\mathbf{v}_t) - \mathbf{F}_{ext,t} = 0 \ , \quad (3)$$

where $\mathbf{F}_{\text{int},t}$ and $\mathbf{F}_{ext,t}$ are the internal and external forces in 3D SBM, respectively. $\mathbf{F}_{\text{int},t}$ is caused by the deformations of zero-length springs in the design domain and calculated as $\mathbf{F}_{\text{int},t} = dU_t / d\mathbf{v}_t$, where U_t indicates the stored elastic energy in design domain from springs. The external force is applied in the opposite direction to target motion and is intentionally introduced to apply the mechanism analysis in the following subsection. For further details, refer to Yu et al. [9].

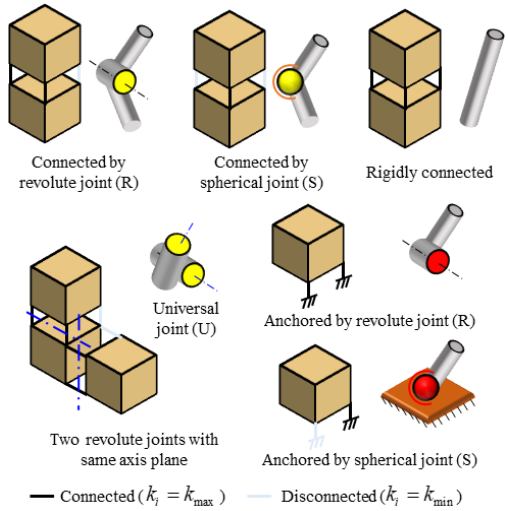

Figure 2. Connections between adjacent 3D blocks through joint types.

B. *Screening for fully rotatable spatial linkage mechanisms*

With the randomly generated values of ξ^K and ξ^X, we can obtain many spatial linkage mechanisms with different configurations and their generating 3D motions. However, not all randomly produced spatial mechanisms will have full rotatability. To filter these out, we utilize the criterion using the mean value of the work transmittance efficiency function ($\bar{\eta}$) used in Yim et al. [15] as follows:

$$1 - \bar{\eta} << \varepsilon = 0.01, \quad (4)$$

where the work transmittance efficiency function (η_t) is the ratio between the input work ($W_{inp,t}$) from the input motor and output work ($W_{out,t}$) by external force [6] at a certain time t:

$$\eta_t = \frac{W_{out,t}}{W_{inp,t}} = \frac{W_{out,t}}{W_{out,t} + U_t} . \quad (5)$$

$W_{inp,t}$ and $W_{out,t}$ can be calculated by the external force $\mathbf{F}_{ext,t}$ applied to the end effector. Earlier work [6] demonstrated that if $1 - \bar{\eta} = 0$ (minimum value), its corresponding mechanism is fully rotatable with a single driving actuator. Theoretically, the tolerance error ε is zero. However, we used $\varepsilon = 0.01$ to permit several numerical tolerances. Therefore, we can generate various fully rotatable spatial linkage mechanisms with the above criterion with randomly generated 3D SBM design variables.

C. *Mechanism dataset for neural network*

With the mechanism dataset generated in Section II B, we constructed a neural network to determine the mechanism topology (initial configuration) when the target 3D motion is given. To this end, the input vector of the mechanism data should represent the characteristic of 3D motion, and the output vector should represent the mechanism topology (initial configuration). To represent the characteristics of the 2D path in the neural network-based method, Yim et al. [15] used Fourier-transformed descriptors of the centroid distance function from the 2D path, which appears to effectively represent the generating path with the topology of the planar mechanism [9, 15, 18]; thus, we also used Fourier transformed descriptors to represent the 3D motions in this study. However, because the centroid distance function cannot be defined as 3D motion, we used three projected 2D paths by projecting 3D motion onto three orthogonal planes, as shown in the upper left of Fig. 1. As in a previous study [15], we used 15$^{\text{th}}$-Fourier-transformed descriptors ($\mathbf{C}$) from three projected target 3D motions, which can be defined as:

$$\mathbf{C} = \begin{bmatrix} a_0^{xy}, \cdots, a_{15}^{xy}, b_1^{xy}, \cdots, b_{15}^{xy}, \\ a_0^{yz}, \cdots, a_{15}^{yz}, b_1^{yz}, \cdots, b_{15}^{yz}, \\ a_0^{zx}, \cdots, a_{15}^{zx}, b_1^{zx}, \cdots, b_{15}^{zx} \end{bmatrix}. \quad (6)$$

The mechanism topology (configuration) can represent a topology design variable ξ^K in 3D SBM. In early literature, topology design variables were used for the output vectors of neural networks. However, based on prior experience, 3D SBM is unable to construct a neural network that directly interpolates topology design variables (the accuracy of the trained neural network did not exceed 32% with the previous method), as it is more complex to represent the mechanism topology (e.g., the same joints can have different rotating axes). This complexity of 3D SBM also affects the accuracy of further neural networks, as discussed in Section III A. Therefore, we defined the natural number as a topology class number (M_T) corresponding to the value of ξ^K sorted in ascending order from all 2 × 2 × 2 3D SBM to make the neural network a multi-class classification problem. Therefore, we can represent the 3D motion as a vector $\mathbf{C}$ of size 93 × 1 and the mechanism topology as the natural number by topology class number (M_T).

With the method in Sections II B and C, we obtained 4,200,000 mechanism datasets. To prevent repetition from rotating the mechanism itself, the input motion was fixed to the *x*-axis and block 1. As a result, in the randomly generated

dataset from 2 × 2 × 2 3D SBM, M_T is between 1 and 97, that is, there are 97 different ξ^K combinations with different configurations of fully rotatable spatial mechanisms.

III. Mechanism Synthesis Process

Our proposed mechanism synthesis process is a two-step approach, as depicted in Fig. 1. The first topology synthesis step determines mechanism topology (M_T) using a pretrained neural network. The mechanism dimensions (ξ^X) are then determined through gradient-based shape optimization in the following dimensional synthesis step.

A. Topology synthesis step with neural network

In the first topology synthesis step, a neural network is used to obtain M_T of the mechanism from a given target $\mathbf{C}$. In this study, we used Resnet-50 with CBAM [19] by changing 2D convolution to 3D convolution for classifying M_T from the input vector $\mathbf{C}$. Among the 4,200,000 mechanism datasets, 4,000,000 were used for training the neural network, and the remaining 200,000 were used for the test. As a trained result, the neural network predicts M_T with an accuracy rate of 78.2% from the input vector $\mathbf{C}$ from the test dataset. The relatively low accuracy of 78.2% appears to be unavoidable due to high nonlinearity in the motions of mechanisms and strong similarity among the motions even when mechanism topologies are different. However, shape optimization reveals that many of the remaining 21.8% (inaccurate mechanisms) generate the desired paths after shape optimization. This is because the same path (within the allowed tolerance error) can be generated by mechanisms of different topologies. This also supports the necessity of performing the shape optimization following the determination of the mechanism's topology. The relevant discussions will be given in Section IV B.

B. Dimensional synthesis step with the gradient-based method

After M_T is determined from $\mathbf{C}$ in the topology synthesis step, the next step is to obtain the link dimensions based on the predetermined mechanism topology. Note that the determination of M_T means the corresponding ξ^K is determined. With a fixed ξ^K, we can consider the mechanism dimension as ξ^X through shape optimization. The optimization problem to determine ξ^X is established as follows:

$$\begin{aligned} &\underset{\xi^X \in \mathbf{R}^{N_s}}{\text{Minimize}} \ \ 1-\bar{\eta} \\ &\text{subject to } \left\| X_t - X_{t,des} \right\| \le \varepsilon \ \ (t=1,2,\cdots,T) \\ &\qquad\qquad \left\| Y_t - Y_{t,des} \right\| \le \varepsilon \ \ (t=1,2,\cdots,T) \\ &\qquad\qquad \left\| Z_t - Z_{t,des} \right\| \le \varepsilon \ \ (t=1,2,\cdots,T) \end{aligned} \quad , \tag{7}$$

where T is the total time step, and N_s is the number of shape design variables. Here, $\bar{\eta}$ is the mean value of the work transmittance efficiency function, and X_t, Y_t, and Z_t ($X_{t,des}$, $Y_{t,des}$, and $Z_{t,des}$) are the global coordinated generating (target) 3D motions. The optimization problem established in (7) was solved by the method of moving asymptotes [20]. More details can be found in literature [17].

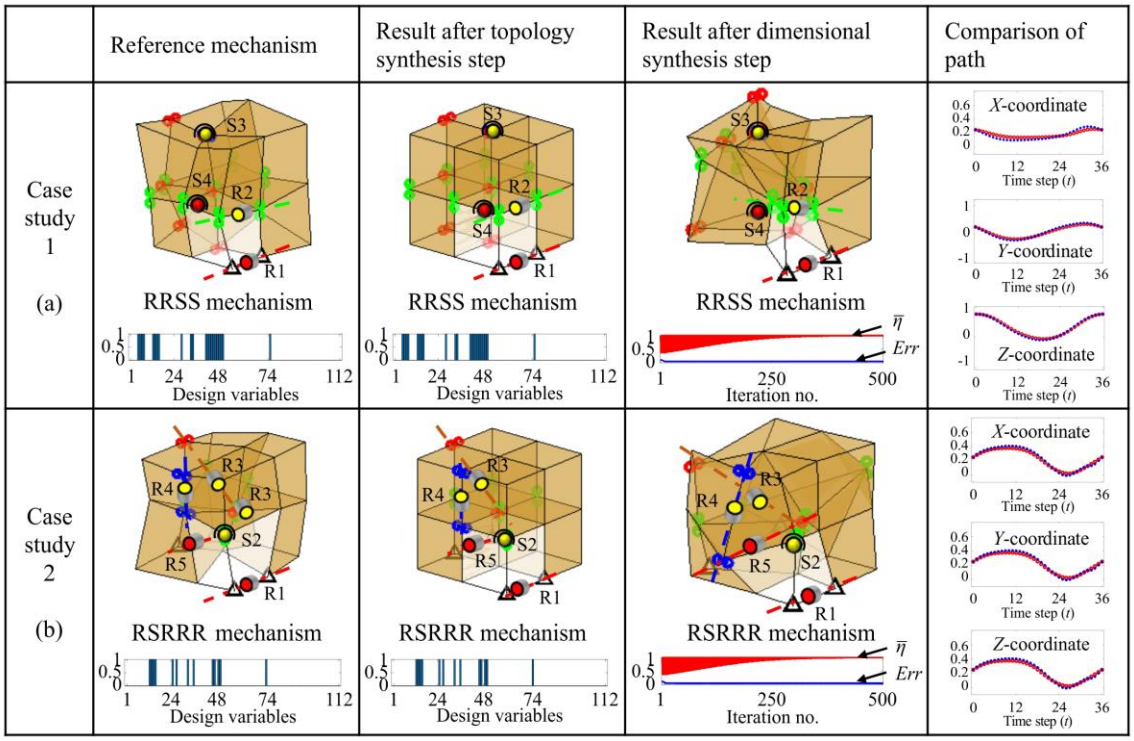

Figure 3 Two case studies with target motions from the already-known mechanisms: (a) in Case Study 1 a RRSS spatial mechanism is synthesized and (b) in Case Study 2 a RSRRR spatial mechanism is synthesized. In the fourth column, red dot is the target motion and blue crossed dot is the generating motion.

IV. SYNTHESIS PROBLEMS FOR THE PROPOSED METHOD

This section reviews several case studies that were conducted using the proposed method. We used the identical trained neural network from Section III for all problems, and the parameters were set throughout the entire process as follows:

$$k_{\max} = 10^4,\ \varepsilon = 0.05,\ \xi^K_{\min} = 10^{-3},\ \xi^X_{\min} = 10^{-2},\ T = 36 \quad (8)$$

During the dimensional synthesis step, the initial design variable $\xi^X = 0.5$ is used to avoid a biased condition. The values in (8) and the initial design variable condition were effective design conditions in earlier topology optimization synthesis problems [15, 17].

A. Mechanism synthesis problems with 3D motions

In this section, two case studies are described on two reference spatial mechanisms (RRSS and RSRRR spatial mechanisms shown in the first column of Fig. 3) that do not belong to the 4,200,000 datasets mentioned in Section III to ensure that the proposed method can successfully synthesize the spatial mechanism with a given target motion from known reference mechanism. In the second column, it can be confirmed that the RRSS and RSRRR spatial mechanisms were synthesized after applying the topology synthesis step. The topology design variables (ξ^K) corresponding to the topology class numbers (M_T) determined during the topology synthesis step are displayed in the same column. The topology design variables in the first and second columns are the same, indicating that a mechanism topology (initial configuration) consistent with the reference mechanism from the topology synthesis step is obtained. After performing dimension synthesis (Step 2), the synthesized mechanism and its optimization history were plotted, as seen in the third column. The comparison between the target and generating motions of the synthesized mechanisms is shown in the fourth column. The synthesized mechanisms successfully trace the target motions with the same topologies (RRSS and RSRRR spatial mechanisms) as the reference mechanisms. With the success of two mechanism synthesis problems with different topologies, it can be said that our proposed method can synthesize a topology of spatial mechanisms for a given target motion.

Next, we will discuss the efficiency of the proposed method based on computational cost compared to previous methods that simultaneously determine topology and shape design variables with 3D SBM. While it is clear that a substantial computational cost is required for neural network construction, the actual synthesis is productive because, once constructed, the neural network can be used equally for various motion-generated synthesis problems. To prove the effectiveness of the proposed method regarding computational cost, we compare the total number of iterations and CPU times with the previous method [17], as shown in Fig. 4, considering a synthesis problem of the same target 3D motion (synthesis details are skipped here). As seen from the figure, once the desired neural network is built, the computational cost of the actual mechanism synthesis process is greatly reduced. The existing synthesis method is a gradient-based optimization problem consisting of 193 design variables, including 112 for topology and 81 for shape design variables. By contrast, in the proposed method, 112 topology design variables are already determined by the topology synthesis step. Due to the high computational cost for neural network construction, the proposed method looks less inefficient in terms of computational cost than the previous method. However, once big data mechanisms are established, the current method may be advantageous because the results are difficult to achieve via other methods.

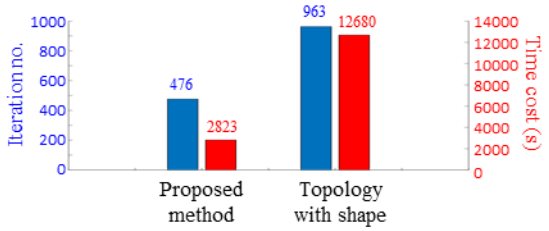

Figure 4. Comparison of the proposed and previous methods of simultaneously determining the topology and shapes in Ref. [17] regarding computational cost and iteration number.

B. Explanation of training accuracy

The neural network proposed in Section III correctly classified the topology class number (M_T) for approximately 78.2% of the test dataset. In this case, and in the cases in Section IV A, the spatial mechanism can be effectively synthesized. However, the 78.2% accuracy of the dataset appears to be inefficient for use in this trained neural network. In this section, we discuss the validity of using trained neural networks despite not having a high accuracy. To this end, we explain that not all the failed 21.8% results are useless because the generated target motion **C** can be synthesized with different mechanism configurations. This is because, if the link dimensions are adjusted appropriately, similar motions can be generated by the different topologies of mechanisms. In addition, in the case of 3D SBM, this phenomenon occurs more frequently because there are several symmetrical spatial mechanisms in a 3D SBM discretized design domain. Thus, the proposed method can design a spatial mechanism that generates the desired motion.

To demonstrate this phenomenon, we prepared the mechanism synthesis problem given in Fig. 5. Fig. 5(a) shows a reference RURS mechanism with 3D SBM and its target motion (red dots in Fig. 5(c)), which will be used as the target motion in the subsequent synthesis problem. After the topology synthesis step with target motion, a configuration with topology design variables different from the reference mechanism is synthesized; however, the synthesized mechanism's topology is the RURS mechanism. Only the angle of the R3 joint (revolute joint) is different from the reference mechanism (see the 27th and 28th design variables). However, in the case of different topology design variables, the generating motion next to the dimensional synthesis step traces the target motion well, as shown in Fig. 5(c).

Further data analysis was performed on the dataset to support the results described above. We plotted all generating motions from the test dataset into the two principal component analysis (PCA) axes, as shown in Fig. 6(c) (colors indicate various M_T values). The detailed process of obtaining PCA axes can be found in earlier literature [15]. For all generating

motions with M_T^{ref} configuration from the test dataset, as shown in Fig. 6(a) (similar to the RURS mechanism in Fig. 5(a)), the M_T^{pred} values were obtained through the topology synthesis step and depicted in Fig 6(b) (similar to Fig. 5(b)). As illustrated in Fig. 6(b), all of the M_T^{pred} have the same anchored spherical joints at the same position, and such an anchoring position may directly affect the generating motion of the spatial mechanism. Among the PCA transformed data in Fig. 6(c), mechanism data are gathered corresponding to the reference topology M_T^{ref} (red dot) and another topology M_T^{pred} dataset, as shown in Fig. 6(d) (the corresponding colors are shown in Fig. 6(b)). The generating motion from M_T^{ref} (red dot) is close to the generating motion from the other topology class numbers M_T^{pred}, which means each M_T^{ref} and M_T^{pred} can generate similar 3D motions. This result causes the training dataset to appear less accurate. However, as in Fig. 5, we can synthesize the spatial mechanism by adjusting the dimension from the spatial mechanisms with different M_T^{pred} values.

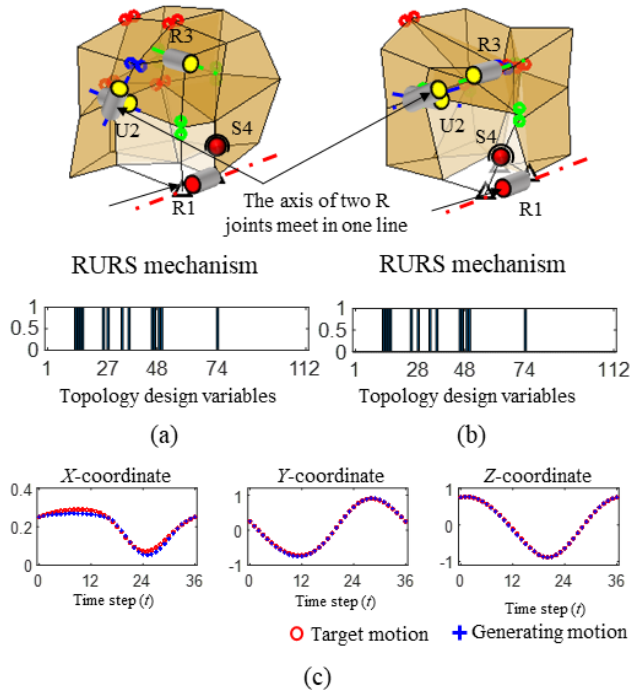

Figure 5. Illustrative synthesis example of failed 21.8% of the test dataset synthesizing the spatial mechanism: (a) reference mechanism; (b) synthesized mechanism; (c) generating motion with the target motion.

Obviously, using a deeper and more complex network can achieve higher accuracy, but this would require more mechanism datasets and computational costs to train. However, shape optimization can cover a certain level of accuracy in the proposed method, which means that mechanism synthesis methods that simultaneously construct big data-based and gradient-based methods are highly efficient. For the above reasons, no further parameter study was conducted to build a highly efficient neural network.

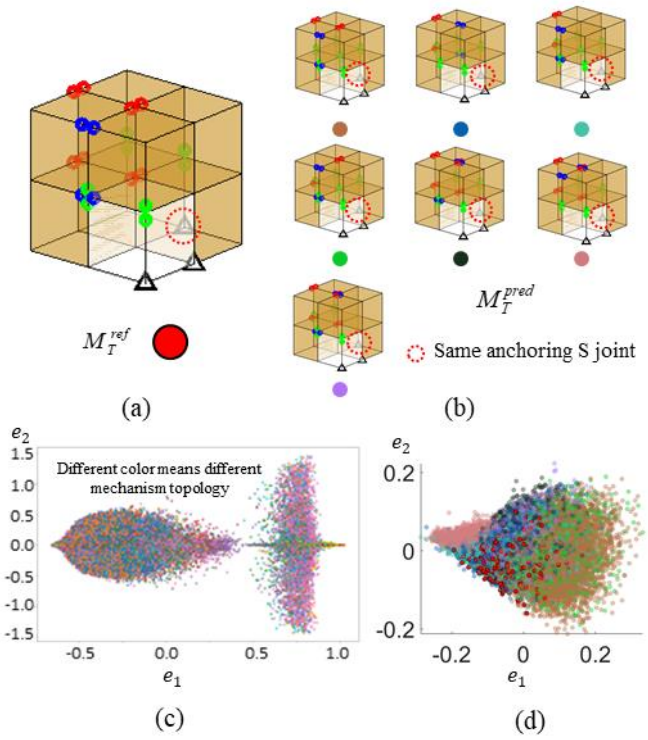

Figure 6. (a) Topology of the reference mechanism in Fig. 5(a); (b) all topology results after the topology synthesis step with all the target motions having the same topology as (a); (c) PCA axes of all test datasets and compiled PCA axes data; (d) with topology (a) and (b).

V. Conclusion

This study proposed a two-step approach to synthesize the topology and dimensions of spatial mechanisms when providing the target motion. This two-step approach, which incorporates a big data approach to determine the mechanism topology and a gradient-based optimization to specify the dimensions, is efficient in reducing computational cost and synthesis difficulty. Additionally, methods of replacing the mechanism topology synthesis problem with multi-class classification have been found to be efficient due to the difficulty of describing the topology of spatial mechanisms. For this reason, we can synthesize the spatial mechanism with less computation cost compared to existing synthesis method.

Despite the success of spatial mechanism topology and dimensional synthesis, especially RRSS, RSRR and RURS spatial mechanisms, there are several limitations that need to be resolved before applying in real-world synthesis problems. First, we simply tested known mechanisms. As a result, we must apply the proposed method to solve real-world design problems that outperform existing mechanisms. If the present analysis focused on the synthesis of complete-path-generation mechanisms is extended further, one should be able to synthesize mechanisms of open and multi-loop paths. Despite some problems to overcome, this method is expected to open a novel approach to designing spatial mechanisms.

REFERENCES

[1] J. J. Cervantes-Sánchez, M. A. Moreno-Báez, L. A. Aguilera-Cortés, and E. J. González-Galván, "Kinematic design of the RSSR-SC spatial linkage based on rotatability conditions," *Mechanism and Machine Theory*, vol. 40, no. 10, pp. 1126–1144, 2005.

[2] J. Chu and J. Sun, "A new approach to dimension synthesis of spatial four-bar linkage through numerical atlas method," *Journal of Mechanisms and Robotics,* vol. 2, p. 041004, 2010.

[3] J. J. Cervantes-Sánchez, L. Gracia, E. Alba-Ruiz, and J. M. Rico-Martínez, "Synthesis of a special RPSPR spatial linkage function generator for six precision points," *Mechanism and Machine Theory*, vol. 46, no. 2, pp. 83–96, 2011.

[4] Y. Lu and T. Leinonen, "Type synthesis of unified planar–spatial mechanisms by systematic linkage and topology matrix-graph technique," *Mechanism and Machine Theory*, vol. 40, no. 10, pp. 1145–1163, 2005.

[5] Y. Lu, L. Ding, and J. Yu, "Autoderivation of topological graphs for type synthesis of planar 3DOF parallel mechanisms," *J. Mechanisms Robotics,* vol. 2, no. 1, p. 011002, 2010.

[6] S. I. Kim and Y. Y. Kim, "Topology optimization of planar linkage mechanisms," *International Journal for Numerical Methods in Engineering*, vol. 98, no. 4, pp. 265–286, 2014.

[7] S. I. Kim, S. W. Kang, Y.-S. Yi, J. Park, and Y. Y. Kim, "Topology optimization of vehicle rear suspension mechanisms," *International Journal for Numerical Methods in Engineering*, vol. 113, no. 8, pp. 1412–1433, 2018.

[8] S. I. Kim, D. Shin, S. M. Han, S. W. Kang, S. Kwon, Y.-S. Yi, and Y. Y. Kim, "A novel space-constrained vehicle suspension mechanism synthesized by a systematic design process employing topology optimization," *Structural and Multidisciplinary Optimization*, vol. 62, no. 3, pp. 1497–1517, 2020.

[9] J. Yu, S. M. Han, and Y. Y. Kim, "Simultaneous shape and topology optimization of planar linkage mechanisms based on the spring-connected rigid block model," *Journal of Mechanical Design*, vol. 142, no. 1, p. 011401, 2020.

[10] S. W. Kang and Y. Y. Kim, "Unified topology and joint types optimization of general planar linkage mechanisms," *Structural and Multidisciplinary Optimization*, vol. 57, no. 5, pp. 1955–1983, 2018.

[11] Y. Y. Kim, G.-W. Jang, J. H. Park, J. S. Hyun, and S. J. Nam, "Automatic synthesis of a planar linkage mechanism with revolute joints by using spring-connected rigid block models," *Journal of Mechanical Design,* vol. 129, no. 9, pp. 930–940, 2007.

[12] S. W. Kang, S. I. Kim, and Y. Y. Kim, "Topology optimization of planar linkage systems involving general joint types," *Mechanism and Machine Theory*, vol. 104, pp. 130–160, 2016.

[13] N. H. Yim, S. W. Kang, and Y. Y. Kim, "Topology optimization of planar gear-linkage mechanisms," *Journal of Mechanical Design*, vol. 141, no. 3, pp. 032301–3230118, 2019.

[14] S. M. Han and Y. Y. Kim, "Topology optimization of linkage mechanisms simultaneously considering both kinematic and compliance characteristics," *Journal of Mechanical Design*, vol. 143, no. 6, p. 061704, 2021.

[15] N. H. Yim, J. Lee, J. Kim, and Y. Y. Kim, "Big data approach for the simultaneous determination of the topology and end-effector location of a planar linkage mechanism," *Mechanism and Machine Theory*, vol. 163, p. 104375, 2021.

[16] A. Kawamoto, M. P. Bendsøe, and O. Sigmund, "Articulated mechanism design with a degree of freedom constraint," *International Journal for Numerical Methods in Engineering*, vol. 61, no. 9, pp. 1520–1545, 2004.

[17] S. M. Han, ″Unified Topology and Shape Optimization of Linkage Mechanisms Simultaneously Considering Kinematic and Compliance Characteristics,″ Thesis, Seoul National University Graduate School, 2020.

[18] S. M. Han, S. I. Kim, and Y. Y. Kim, "Topology optimization of planar linkage mechanisms for path generation without prescribed timing," *Structural and Multidisciplinary Optimization*, vol. 56, no. 2, pp. 1–17, 2017.

[19] S. Woo, J. Park, J.-Y. Lee, and I. S. Kweon, "CBAM: Convolutional block attention module," *European Conference on Computer Vision*, pp. 3–19.

[20] K. Svanberg, "The method of moving asymptotes—a new method for structural optimization*," International Journal for Numerical Methods in Engineering*, vol. 24, no. 2, pp. 359–373, 1987.